AIP Applied Physics Letters

Ge nanocrystals in SiO 2 films

Takamitsu Kobayashi, Toshiaki Endoh, Hisashi Fukuda, Shigeru Nomura, Akira Sakai, and Yuji Ueda

Citation: Applied Physics Letters **71**, 1195 (1997); doi: 10.1063/1.119623
View online: http://dx.doi.org/10.1063/1.119623
View Table of Contents: http://scitation.aip.org/content/aip/journal/apl/71/9?ver=pdfcov
Published by the AIP Publishing

Ge nanocrystals in SiO_2 films

Takamitsu Kobayashi, Toshiaki Endoh, Hisashi Fukuda,[a] Shigeru Nomura, Akira Sakai, and Yuji Ueda
Department of Electrical and Electronic Engineering, Faculty of Engineering, Muroran Institute of Technology, 27-1 Mizumoto, Muroran, Hokkaido 050, Japan

(Received 29 April 1997; accepted for publication 26 June 1997)

SiO_2/Ge nanocrystal/SiO_2 structures have been fabricated by deposition of Ge film on a SiO_2 layer and subsequent oxidation of the structure at a temperature between 800 °C and 1000 °C. Secondary ion mass spectrometry results indicate that the Ge precipitates into the bulk SiO_2 at a density of 1×10^{12} cm^{-2}. Raman spectra show a sharp peak at 300 cm^{-1} for the nanocrystallized Ge. The nanocrystal diameter is determined to be 5 nm on average. In the metal–insulator–silicon structure, electron storage occurs in the SiO_2/Ge/SiO_2 potential well via electron tunneling into the oxide film. Capacitance-voltage measurements indicate that flatband voltage (V_{FB}) shifts to 0.91 V after the electron injection. The V_{FB} shift is attributed to the charge storing for a single electron per potential well. © *1997 American Institute of Physics.* [S0003-6951(97)01035-8]

During the past few years, a considerable amount of attention has been focused on the strong photoluminescence (PL) in the visible wavelength range from nanostructures made of group IV elements, such as porous Si,[1,2] Si,[3,4] and Ge[5–7] nanocrystals prepared by various methods. To obtain three dimensionally confirmed systems, several groups have experimented with various techniques, for example, pyrolysis,[8,9] cosputtering,[5,10,11] pulsed-laser ablation,[12] spark processing,[13] and ion implantation.[14] For the Ge nanocrystals, most reports of visible PL from low-dimensional structures have involved Ge nanocrystals embedded in SiO_2. To our knowledge, although the optical properties of these nanostructures have been extensively investigated, there are few studies on their electrical properties. Recent reports have been focused on room-temperature observation of negative differential conductance in a structure consisting of a SiC/Si/SiC[15] or SiO_2/Si/SiO_2[16] matrix. For the SiO_2/Si/SiO_2 system, the anomalous steps in the current-voltage ($I-V$) characteristics have been described.[17]

In this study, we fabricated Ge nanocrystals embedded in a SiO_2 matrix, and evaluated the crystallinity, distribution and electrical properties of the SiO_2/Ge nanocrystal/SiO_2 structure. The Ge crystals of nanometer size were obtained using the conventional silicon fabrication process which is the primary process of the integrated circuit industry.

In the growth of the Ge nanocrystals in the SiO_2 film, 4-nm-thick tunnel SiO_2 film was first grown on a p-type 1–2 Ω cm Si (100) substrate in a dry oxygen (O_2) ambient at 900 °C for 5 min. Then, 10-nm-thick Ge film was deposited on the tunnel oxide using electron-beam evaporation at a substrate temperature of 60 °C and a base pressure of 2×10^{-7} Torr. The Ge layer was then annealed a temperature between 800 and 1000 °C for 1 h in a dry O_2 ambient. It is believed that due to the rapid diffusion of O_2 molecules through the Ge grain boundaries, the Ge became crystallized and embedded in the SiO_2 during high temperature oxidation. The total film thickness of the SiO_2 layer was 20 nm, determined by ellipsometry with a fixed refractive index of 1.460. The depth profile of Ge in the SiO_2 film was evaluated by secondary ion mass spectrometry (SIMS) using O_2^+ as a primary ion at 8 keV. Raman spectra were obtained using the 496.5 nm line of an Ar^+ laser as the excitation source. A cooled photomultimeter tube and photon counting electronics interfaced to a microcomputer were used to collect and analyze the data. For electrical measurements, aluminium (Al) gate electrodes (0.1 mm ϕ) were deposited after etching away of the SiO_2 on the wafer backside. An automatic semiconductor parameter analyzer was used in the capacitance-voltage ($C-V$) measurements of the metal–insulator–semiconductor (MIS) structures.

Typical SIMS depth profiles of Ge in the SiO_2 films are shown in Fig. 1. The Ge depth profiles seemed to be strongly dependent on the oxidation temperature. For the oxidation at 800 °C, Ge remains at the surface of the oxide with a small hump in the bulk oxide. In contrast, Ge near the surface of the oxide disappears upon oxidation at 1000 °C. In addition, the maximum concentration of Ge (2×10^{18} atoms/cm^3) is

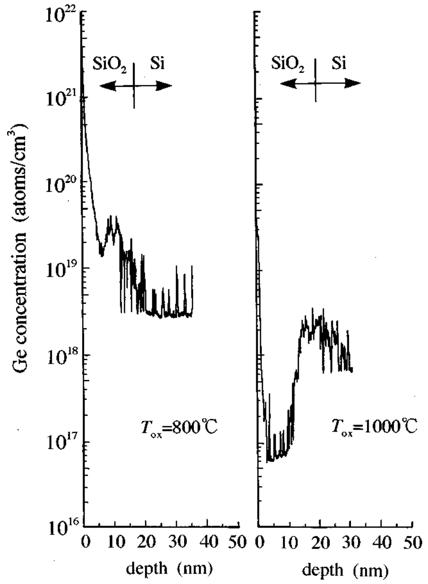

FIG. 1. The depth profiles of Ge in SiO_2 films after oxidation at 800 and 1000 °C.

---

[a] Electronic mail: fukuda@waspet.cc.muroran-it.ac.jp

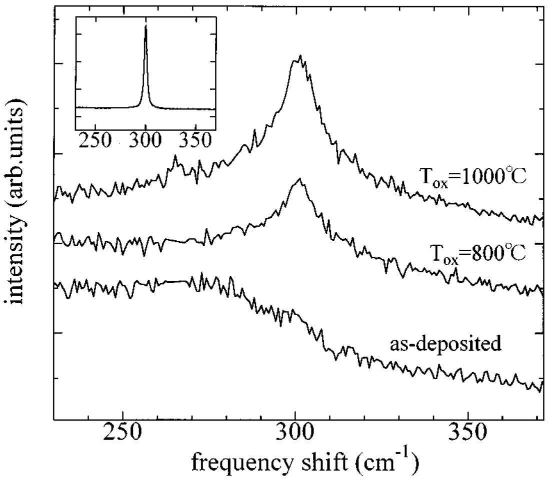

FIG. 2. Raman spectra for Ge layers as-deposited and oxidized at 800 and 1000 °C. The inset shows a Raman spectrum for unstrained Ge sample.

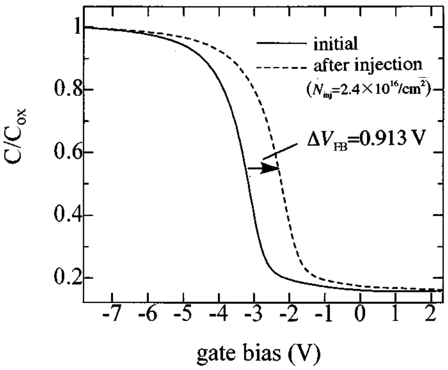

FIG. 3. Capacitance-voltage curves for the initial state and after electrons at $N_{\mathrm{inj}}=2.4\times10^{16}$/cm^2 were injected.

found near the $\mathrm{SiO_2}$/Si interface for the 1000 °C annealed sample. In our experiment, the Ge layer was initially deposited on a 4-nm-thick $\mathrm{SiO_2}$ layer on a Si substrate, and then oxidized at a high temperature. It is interesting that diffusion of Ge in the $\mathrm{SiO_2}$ layers is minimal during the oxidation. Moreover, a rapid nucleation of Ge occurs depending on the oxidation temperature. In oxidation at 800 °C, which is below the melting temperature of Ge (938.3 °C), the Ge nucleation process is in a period of transition where the Ge remains near the top oxide layer. With increasing oxidation temperature, Ge precipitates in the bulk $\mathrm{SiO_2}$ layer, as shown in Fig. 1. The out-diffusion of Si from the substrate could influence the Ge nucleation and growth processes. It has been reported that the diffusion of Si atoms from the substrate enhances the precipitation of Ge in $\mathrm{SiO_2}$.[18] It is known that Ge oxide is thermodynamically less stable than $\mathrm{SiO_2}$.[19] Therefore, it should be easier for Ge than for Si to precipitate in $\mathrm{SiO_2}$. However, further investigation on the specific distribution of Ge nucleation sites after oxidation is required.

We measured Raman spectra for as-deposited and oxidized samples to determine the size of the Ge nanocrystals formed in $\mathrm{SiO_2}$. As shown in Fig. 2, the Raman spectrum of the as-deposited sample has a broad peak at around 270 cm^{-1} attributed to the amorphous Ge–Ge mode. The crystallization of the amorphous Ge is evidenced by the narrowing and disappearance of the broad peak at around 270 cm^{-1} and the onset of the sharp $\Gamma_{25'}$ phonon peak at around 300 cm^{-1} for the oxidized samples. In the Raman spectra of the bulk unstrained Ge crystals, the Ge–Ge peak is symmetric and centered at 300.5 cm^{-1} with a full width at half maximum (FWHM) of 2.7 cm^{-1}. The peak intensity ratio of the unstrained Ge to nanocrystalline Ge in $\mathrm{SiO_2}$ was 18:1. With increasing oxidation temperature, a sharp Raman peak with an asymmetric shoulder at the low frequency side is found, as shown in Fig. 2. The average particle size was determined by use of a model of the Raman line shape of semiconductor nanocrystals, in which the half width of the maximum peak[18] and the peak shift[20] of the Raman peak are fitted to the data. The size of the Ge nanocrystals embedded in the $\mathrm{SiO_2}$ is estimated to be 5 nm on average. The size of the Ge nanocrystals is in good agreement with the results reported elsewhere in the previous literature.[18,20]

The multiple confinement of free carriers in quantum wells has led to several significant observations of physical phenomena and demonstrations of the usefulness of in electronic and optoelectronic devices. $C-V$ measurement before and after forward constant voltage (V_{ap}) stress was used to investigate charge storage in the Ge nanocrystals. As shown in Fig. 3, a positive voltage shift in the $C-V$ curve is observed upon electron injection at $N_{\mathrm{inj}}=2.4\times10^{16}$/cm^2 with application of a bias of $V_{ap}=15$ V. No flatband voltage shift (ΔV_{FB}) occurs upon electron injection in MIS capacitors without Ge nanocrystal in $\mathrm{SiO_2}$. Moreover, no distortion of the $C-V$ curve after the injection due to of interface-trapped charge is observed. The number of electrons (N_{inj}) that were injected into the oxide during stress was calculated by integration of the injected gate current density I_{ap} at constant stress voltage V_{ap} over the injection time. ΔV_{FB} is defined as the flatband voltage point in the $C-V$ curve measured between the initial state and after the electron injection. After the electron injection, V_{FB} shifts to 0.91 V, in a positive direction. This means that the negative charge buildup into $\mathrm{SiO_2}$ occurs due to electron tunneling in electron traps from the substrate. If the charge buildup is significant, the experimental $C-V$ curve will be shifted from the ideal theoretical curve, in which the magnitude of ΔV_{FB} for a single electron per nanocrystal is approximately given by[21]

$$\Delta V_{\mathrm{FB}}=\frac{qn_{\mathrm{well}}}{\epsilon_{\mathrm{ox}}}\left(t_{\mathrm{ox}}+\frac{\epsilon_{\mathrm{ox}}t_{\mathrm{well}}}{2\epsilon_{\mathrm{Si}}}\right), \qquad (1)$$

where t_{ox} is the thickness of the oxide under the gate, t_{well} is the linear dimension of the nanocrystal well, ϵ's are the permittivities, q is the magnitude of the electronic charge, and n_{well} is the density of the nanocrystals. For the 5-nm-diam Ge nanocrystals located, i.e., a nanocrystal density of 1×10^{12} cm^{-2} as estimated by SIMS, and an oxide thickness of 20 nm, the shift is calculated to be 0.9 V for one electron per nanocrystal. This value is in good agreement with the ΔV_{FB} determined from the $C-V$ curves. The Coulomb blockade effect can also be very significant at these dimensions. The Coulomb charging energy ($q^2/2C_n$, where C_n is the nanocrystal capacitance) for a 5-nm-diam nanocrystal of Ge in $\mathrm{SiO_2}$ is about 74 meV. Not only is it larger than the thermal energy, but it also limits additional injection of carriers in to the nanocrystal.

In summary, we have fabricated a Ge nanostructure embedded in SiO_2 by deposition of Ge on SiO_2 and subsequent high temperature oxidation. SIMS revealed that the outdiffusion of Ge toward the SiO_2 layer was minimal. At the temperature of 1000 °C, the Ge layer in the SiO_2 grew with a concentration of 1×10^{12} atoms/cm^2. Raman spectra showed that after oxidation the Ge layer precipitated and crystallized in the SiO_2. The $C-V$ measurement results indicate that after the electron injection into SiO_2, electrons are captured in each SiO_2/Ge/SiO_2 quantum well.

This work was supported by the Foundation for the Promotion of Material Science and Technology of Japan (MST Foundation).

[1] L. T. Canham, Appl. Phys. Lett. **57**, 1046 (1990).
[2] V. Lemann and U. Gosele, Appl. Phys. Lett. **58**, 856 (1991).
[3] S. Furukawa and T. Miyasato, Jpn. J. Appl. Phys., Part 2 **27**, L2207 (1989).
[4] D. Zhang, R. M. Kolbas, P. D. Milewski, D. J. Lichtenwalner, A. I. Kingon, and J. M. Zavada, Appl. Phys. Lett. **65**, 2684 (1994).
[5] Y. Maeda, N. Tsukamoto, Y. Yazawa, Y. Kanemitsu, and Y. Matsumoto, Appl. Phys. Lett. **59**, 3168 (1991).
[6] A. K. Dutta, Appl. Phys. Lett. **68**, 1189 (1996).
[7] K. S. Min, K. V. Shcheglov, C. M. Yang, H. A. Atwater, M. L. Brongersma, and A. Polman, Appl. Phys. Lett. **68**, 2511 (1996).
[8] C. B. Murray, D. J. Norris, and M. G. Bawendi, J. Am. Chem. Soc. **115**, 8706 (1993).
[9] K. A. Littau, P. J. Szajowski, A. J. Miller, A. R. Kortan, and L. E. Brus, J. Phys. Chem. **97**, 1224 (1993).
[10] Y. Osaka, K. Tsunetomo, F. Toyomura, H. Myoren, and K. Kohno, Jpn. J. Appl. Phys., Part 2 **31**, L365 (1992).
[11] S. Hayashi, T. Nagareda, Y. Kanzawa, and K. Yamamoto, Jpn. J. Appl. Phys., Part 1 **31**, 3840 (1993).
[12] E. Werwa, A. A. Seraphin, L. A. Chiu, C. Zhou, and K. D. Kolenbrander, Appl. Phys. Lett. **64**, 1821 (1994).
[13] M. H. Ludwig, R. E. Hummel, and S.-S. Chang, J. Vac. Sci. Technol. B **12**, 3023 (1994).
[14] T. Shimizu-Iwayama, K. Fujita, S. Nakao, K. Saitoh, T. Fujita, and N. Itoh, J. Appl. Phys. **75**, 7779 (1994).
[15] E. Fortunato, R. Martins, I. Ferreira, M. Santos, A. Marcario, and L. Guimaraes, J. Non-Cryst. Solids **115**, 120 (1989).
[16] R. Tsu, Quiyi Ye, and E. H. Nicollian, Proc. SPIE **1361**, 232 (1990).
[17] S. Y. Chou and A. E. Gordon, Appl. Phys. Lett. **60**, 1827 (1992).
[18] D. C. Paine, C. Caragianis, and Y. Shigesato, Appl. Phys. Lett. **60**, 2886 (1992).
[19] F. K. LeGoues, R. Rosenberg, T. Nguyen, F. Himpsel, and B. S. Meyerson, J. Appl. Phys. **65**, 21724 (1989).
[20] D. C. Paine, C. Caragianis, T. Y. Kim, Y. Shigesato, and T. Ishahara, Appl. Phys. Lett. **62**, 2842 (1993).
[21] S. Tiwari, F. Rana, H. Hanafi, A. Hartstein, E. F. Crabbe, and K. Chan, Appl. Phys. Lett. **68**, 1377 (1996).